Technology and Advanced Development for a Non-Toxic Orbital Maneuvering System and Reaction Control System for Orbiter Upgrade

NASA Research Announcement 9-NRA-BE-96-1

Contract NAS 8-98042

Non-Toxic Orbiter OMS Engine Technology Program

Final Report

06 January 1999

Prepared For:

National Aeronautics and Space Administration
Marshall Space Flight Center

Prepared by:

W.A. Hayes
Mechanical Design
Mechanical Engineering

V.A. Gibson
Materials and Composites
Mechanical Engineering

F.A. Ferrante
Thermal Analysis
Mechanical Engineering

G.L. Engelmann
Applied Mechanics and Structures
Mechanical Engineering

Approved by:

P.C. Phillipsen
Program Manager
Strategic & Space Propulsion

1.0 Introduction / Summary

NASA intends to pursue technology applications to upgrade the Space Shuttle Orbiter OMS and RCS systems with non-toxic propellants. The primary objectives of an upgraded OMS/RCS are improved safety and reliability, reduced operations and maintenance costs while meeting basic OMS/RCS operational and performance requirements. The OMS/RCS has a high degree of direct interaction with the crew and requires subsystem and components that are compatible with integration into the orbiter vehicle with regard to external mold-line, power and thermal control

The non-toxic propulsion technology is also applicable to future Human Exploration and Development of Space (HEDS) missions. The HEDS missions have similar requirements for attitude control and lander descent/ascent propulsion and which will emphasize the use of In-Situ Resourse for propellants.

When used as a regenerative coolant as in the Shuttle Orbiter OMS combustion chamber, non-toxic fuels such as ethanol are limited in their cooling capacity by the bulk temperature rise permitted to prevent film boiling or possible coking. Typical regeneratively cooled chambers are constructed from highly conductive copper, which maximizes heat transfer, or from low conductivity materials like stainless steel that can also exacerbate cooling problems. For an ethanol cooled application the heat transfer into the fluid must be controlled to reduce the fuel coolant bulk temperature rise. An approach to provide this control is the subject of this report.

This report is being issued to document work done by Aerojet on NASA contract NAS 8-98042. Specifically, this project investigates of the use of ethanol, a designated non-toxic fuel, as a coolant for the Space Shuttle Orbital Maneuvering System Engine combustion chamber. The project also addresses a cost reducing fabrication technique for construction of such a combustion chamber. The study contained three major sub-tasks: an analytical investigation and trade study which included layout of a flight type chamber concept, the fabrication and evaluation of formed platelet liner panels and the preparation and testing of mechanical properties specimens representative of a novel hot gas wall concept.

The analytical trade study was used to identify chamber sizing, contour, coolant channel geometry, and required coolant flowrates. Variables that were considered included available combustion chamber fabrication techniques along with materials of construction. Assumptions made included an anticipated uprated chamber pressure of 175 psi based on on-going studies at NASA, a resultant injector diameter of 7 inches and an L' identical to the baseline, or current, OMS engine. The values of these factors for the current OMS-E are 135psi, 8 inches and 16 inches, respectively.

Results of the trade study identified a composite, or bi-metallic, stainless steel and copper hot gas wall as the most thermally efficient option. Such a configuration is not practical with conventional fabrication techniques. However, this type of construction, though not previously demonstrated, was considered possible with Aerojet's Formed Platelet Liner technology developed and demonstrated under NASA contract NAS 8-37456. This concept was investigated

through the fabrication and evaluation of Formed Platelet Liner panels employing a composite hot gas wall.

The referenced NASA contract demonstrated the viability of the Formed Platelet Liner approach during Phase B, in which a hot fireable chamber was constructed and was test fired at MSFC. The chamber was of the 40k thrust size and utilized an all ZrCu Formed Platelet Liner. A description of the basic Platelet design/fabrication process and that of the Formed Platelet Liner process may be found in Appendix A. Discussion of the testing of the 40k FPL chamber may be found in Reference 3

The Formed Platelet Liner panel demonstration task utilized the basic platelet design and tooling from the original technology development and demonstration phase of the above referenced NASA contract as a means of cost reduction. This tooling, designed for a 40k thrust, 3000 psi H2 / O2 engine, produced panels of a size sufficiently representative of those identified for the Non-Toxic propellant Space Shuttle OMS application.

Multiple panels were fabricated and evaluated during this task; all had the stainless steel / copper composite hot gas walls identified by the analytical trade studies. Two types of panel channel closeouts were produced. One panel type had what has become the traditional design with copper closeout platelets. The other type of panel had a stainless steel closeout platelet. The advantage of this steel closeout approach is that, for low chamber pressure applications as in the OMS pressure fed system, it potentially allows a pressure and axial load carrying capability as an integral part of the Platelet liner. The typical approach to obtaining this load carrying capability is through the subsequent application of a structural jacket, usually by electroforming a layer, or layers, of nickel onto the liner. Elimination of this jacket significantly reduces the complexity of the assembly and provides a means of component and system weight reduction.

Evaluation of the demonstration panels included dimensional inspection, cold flow, dissection, internal feature dimensional inspection, and metallographical evaluation of the diffusion bonds between adjacent platelets. Additionally, mechanical properties specimens, utilizing the same materials of construction and the same processing parameters as the demonstration panels were prepared and tested. The results of these specimen tests provided additions to the Aerojet database on stainless steel to copper diffusion bonds and also provided data on the low cycle fatigue properties of such a bond.

The positive results obtained from the demonstration panel evaluations and mechanical properties testing indicated the concept of the stainless steel / copper composite hot gas wall to be valid. The thermal trade studies provided an analytical prediction of a burn out safety factor of 1.5 achievable with minimum pressure drop. This, coupled with a predicted life well in excess of 1000 cycles, make the Formed Platelet Liner combustion chamber approach extremely attractive as an option for an upgraded Space Shuttle OMS engine with ethanol as the fuel and chamber coolant.

The concept for a flight type version of a non-toxic propellant Space Shuttle OMS engine, developed from the trade studies appears, in Figure 1. The chamber contains a Formed Platelet

Platelet Liner with an integral structural jacket of the type previously described. The concept shown makes use of a scaled version of a low cost injector design developed on Aerojet IR&D during 1998. Such an engine makes use of currently available technologies to produce a lightweight, robust and cost-effective upgrade for a non-toxic OMS-E application.

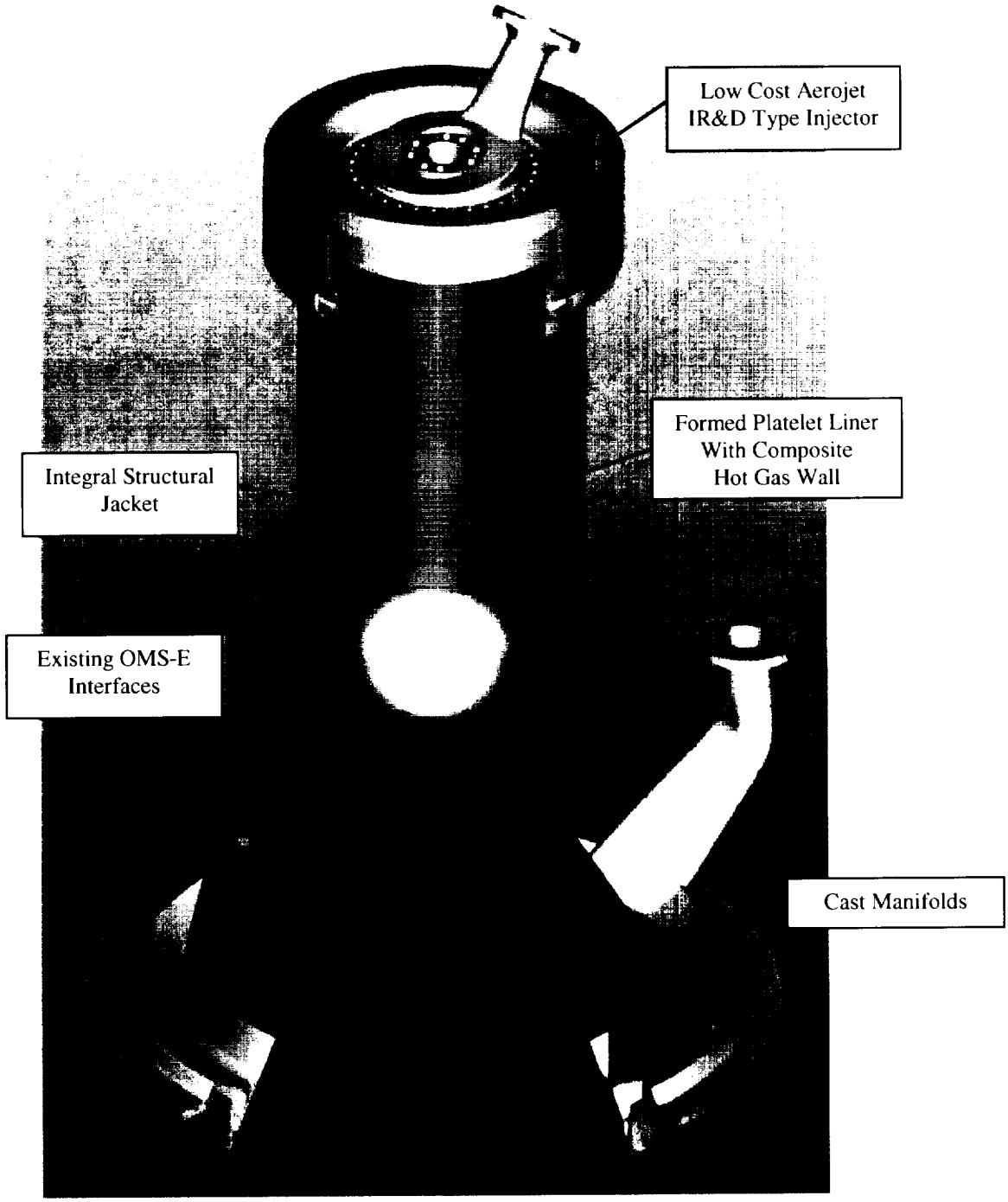

Figure 1. Non-Toxic OMS Engine Concept

2.0 Thermal Analysis / Thermal Design

2.1 Summary

Trade studies were conducted to compare various chamber design concepts for a new Space Shuttle Orbit Maneuvering System (OMS) engine that utilizes a non toxic propellant combination of liquid oxygen and ethanol. Design concepts that were studied were (1) conventional milled slots utilizing stainless steel similar to the current Space Shuttle OMS engine, (2) conventional milled slots utilizing copper, (3) formed platelet liner (FPL) with a stainless steel hot gas wall and copper lands, (4) formed platelet liner with copper hot wall and lands, and (5) formed platelet liner with a hot gas wall composed of stainless steel on the ID and copper on the OD (referred to as a composite hot gas wall) and copper lands. The trade studies showed that the formed platelet liner with a composite hot gas wall is the best option in terms of thermal margin.

2.2 Introduction

The current Space Shuttle OMS engine is a 6000 lbf thrust, pressure fed and has a regeneratively cooled chamber. The propellants used are nitrogen tetroxide as the oxidizer and monomethyl methlyhyrazine (MMH) as the fuel. NASA has a desire to replace the current toxic propellant combination with an non toxic combination namely liquid oxygen and ethanol. The requirement for the propellant replacement is that the new engine maintain the current long life requirement and burnout safety margin. The life requirement is for one thousand starts.

Burnout safety margin refers to the comparison of critical heat flux to the heat flux to the coolant. For subcritical liquid propellants the critical heat flux is the heat flux at which the coolant capability is severely degraded from nucleate boiling to film boiling typically resulting in burnout of the chamber. Since the shuttle is a man rated system successful engine operation is required in over a wide range of propellant inlet conditions. The purpose of this study was to examine various chamber design concepts and chamber materials to determine their feasibility for the non-toxic propellant upgrade.

2.3 Technical Discussion

The burnout heat flux of propellants is typically correlated in terms of the product of coolant velocity and subcooling (coolant saturation temperature minus coolant bulk temperature). The burnout heat flux correlation for MMH is documented in Reference 1. Recent heated tube work done at NASA Lewis correlated the critical heat flux for ethanol (see Reference 2). A comparison of two propellants' critical heat flux versus velocity subcooling product is shown in Figure 1. Ethanol has a lower critical heat than MMH. Figure 2 shows a comparison of the saturation temperature of the two propellants versus pressure. The ethanol has a lower saturation temperature than the MMH. The combination of lower saturation temperature and lower critical heat flux result in a more challenging design for ethanol as coolant as compared to MMH.

Since the Space Shuttle is a man rated system, the engine must operate over a wide range of mixture ratios to account for possible loss of pressurization. At the nominal operating point of the engine the burnout safety factor (ratio of critical heat flux to heat flux of the coolant) is in range of 1.5 to 1.7 depending on the engine. The engine to engine variation is due to two major effects. First, each engine had a slightly different heat flux profile which obviously effected the heat flux to the coolant. Each engine was fired in a heat sink chamber to determine its maximum heat flux profile. The second major effect was the chamber coolant channel flow distribution. Since the critical heat flux varies with coolant velocity and subcooling , a low flow channel would have a lower critical heat flux due to less flowrate and less subcooling due to a higher bulk temperature rise. The relationship of low flow channels to circumferential heat variation causes an engine to engine variability in BOSF.

The gas side heat flux used for the trade studies was modeled with a reactive integral boundary layer model. The gas side heat flux profile was assumed to be similar to the Space Shuttle OMS engine. The nominal fuel bulk temperature rise of the existing Shuttle OMS engine was matched with a model. The model accounts for thermo chemical difference between the existing and non-toxic propellant combination. A ten percent augmentation factor was applied to account for circumferential heat flux variations from nominal.

For this trade study two different chamber concepts and different materials were considered. A conventional milled slot chamber design similar to that used on the existing Space Shuttle OMS engine was one of the concepts studied. The channel and land widths were limited to a minimum of 0.035 inch to represent a conventional milled design. Two different materials stainless steel and copper were studied for this design concept. The other design concept studied was a Formed Platelet Liner (FPL) concept. This design concept is very effective for chamber cooling since it allows for small gas side wall thicknesses and packaging of many channels. For this trade study the channel and land width were limited to a minimum of 0.025 inch although channel and land widths of 0.020 inch have been successfully demonstrated on the 40k FPL program (Reference 3).

For the FPL, three different materials were studied for a hot gas wall thickness. All three FPL design concepts had copper lands and nickel closeout. The material chosen for the closeout has negligible impact on the coolant channel capability. One concept studied had a gas side wall constructed only of stainless steel. The second concept consisted of copper so it was consistent with the successful 40k FPL liner. The third FPL design option consisted of a composite hot gas wall with stainless steel on the ID and copper on the OD forming the channel bottoms. This concept has the advantage of having a higher gas side wall temperature therefore lowering the coolant bulk temperature rise of the propellant while still having copper to permit conduction to the land regions. The platelet configuration pressure drop was based on Advanced Main Combustion Chamber (AMCC) cold flow test data.

The trade studies were done at the nominal operating point which is a mixture ratio of 1.7 and chamber pressure of 175 psia. The fuel inlet pressure was assumed to be 340 psia which represents an approximate increase of 100 psia from the current shuttle. The desired BOSF was 1.5 at nominal operating point to provide some operating range. Gas side boundary conditions were calculated with an Aerojet in-house computer code SCALE. Detailed BOSF calculations were done with a SINDA channel model. The combustion chamber was assumed to mate up with the existing shuttle nozzle so the chamber exit diameter was fixed. The combustion chamber length was taken to be 16" which is approximately the existing shuttle OMS engine. The chamber pressure was assumed to be 175 psia, which provides for better performance due to less kinetics loss and a higher area ratio nozzle. The chamber diameter was assumed to be 7.0 inches.

2.4 Results / Conclusions

The first trade study conducted was to be examine the total propellant heat load. This heat load is important since in the barrel section the coolant bulk temperature is very critical in terms of burnout safety factor. The existing space shuttle OMS engine has propellant heat load of 781 Btu/sec. The heat load increases to 974 BTU/sec using the existing OMS-E engine with lox/ethanol propellant combination. This represents an increase of approximately 25 % and is a result of the higher combustion temperature and thermochemical transport of the combustion products of the non tox propellant combination as compared to the storables. The baseline engine , which has a smaller diameter throat and barrel sections than the current OMS engine, has a heat load to the fuel propellants of 1076 Btu/sec for a stainless steel wall and 1180 Btu/sec for copper gas side wall. A copper wall runs at approximately 400 F whereas a stainless steel would be designed to run at 800 F. This difference results in a 10 percent increase in bulk temperature rise. The results of this trade study are summarized in Table 1.

The results of the BOSF trade study at the throat are shown in Figure 3. For a milled stainless steel chamber operating at a chamber pressure of 175 psia a coolant velocity of 50 fps is required for a BOSF = 1.0. For a BOSF = 1.5 a coolant velocity of greater than 100 fps is required. This high coolant velocity makes the milled stainless steel chamber concept not desirable due to pressure drop limitations. The copper milled and FPL with a stainless steel hot gas wall chamber design concepts require only about 30 fps to achieve a BOSF = 1.5 at the throat. The FPL chamber design concepts with either an all copper hot gas wall or a composite wall have a BOSF over 2 at 30 fps. These design concepts have a slightly different shape of their curves as compared to the other design concepts. The coolant wall temperature with these two design concepts is below the coolant saturation temperature, therefore the propellant is not in nucleate boiling. For these concepts increasing the coolant velocity after a certain point reduces the coolant fin efficiency and coolant surface area resulting in a decreasing BOSF which is typically not expected with increasing coolant velocity.

The coolant velocity versus BOSF trades in the barrel section are in Figure 4. The copper milled chamber design concept requires a coolant velocity of about 40 fps for a BOSF of 1.0 and about 70 fps for a BOSF of 1.5. The FPL with a stainless steel wall and a with all copper wall design concepts show require a coolant velocity about 28 fps for a BOSF of 1.0 and about 50 fps for a BOSF of 1.5. These design concepts are nearly identical in required coolant velocities since the higher thermal conductivity of the all copper gas side wall is offset by the higher propellant bulk temperature due the copper wall. The FPL with a composite wall design only requires a coolant velocity of about 36 fps results in BOSF of 1.5. As a comparison the copper milled deign concept has a BOSF of about 0.9 at the same coolant velocity. The FPL with a composite wall is the superior design concept because it has good thermal conduction near the coolant due to the copper and lower propellant temperature due to the stainless steel near the combustion products.

Name	Wall Material	Q (BTU/sec)	PC (psia)
OMS-E (ST)	SS	781	125
OMS-E (NT)	SS	974	125
BASELINE (NT)	SS	1076	175
BASELINE (NT)	CU	1180	175

BASELINE (DC = 7.0", L'=16", A/R = 70)

SS = STAINLESS STEEL ASSUMED @ 800 F
CU = COPPER ASSUMED @ 400 F
ST = STORABLES (NTO/MMH)
NT = NON TOXIC (LOX/Ethanol)

Table 1. Heat Load Comparison

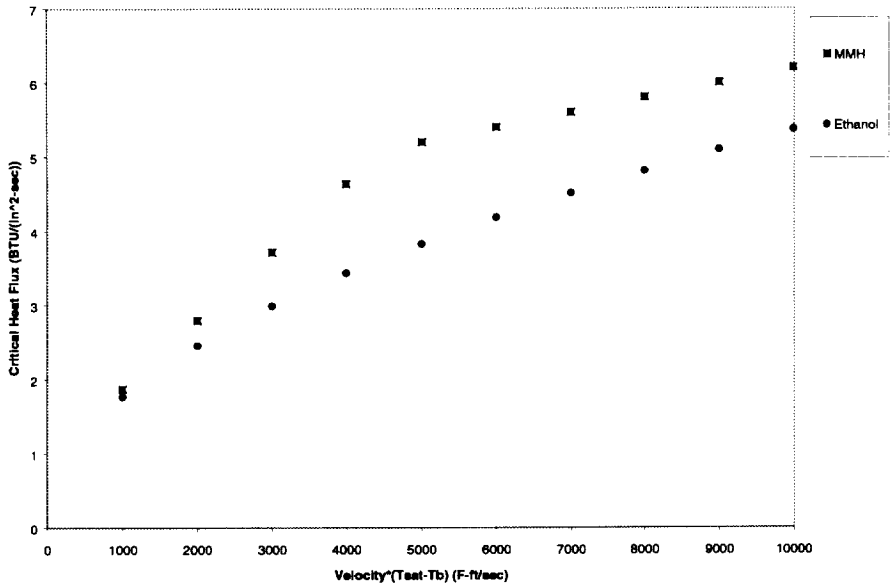

Figure 2. Propellant Critical Heat Flux

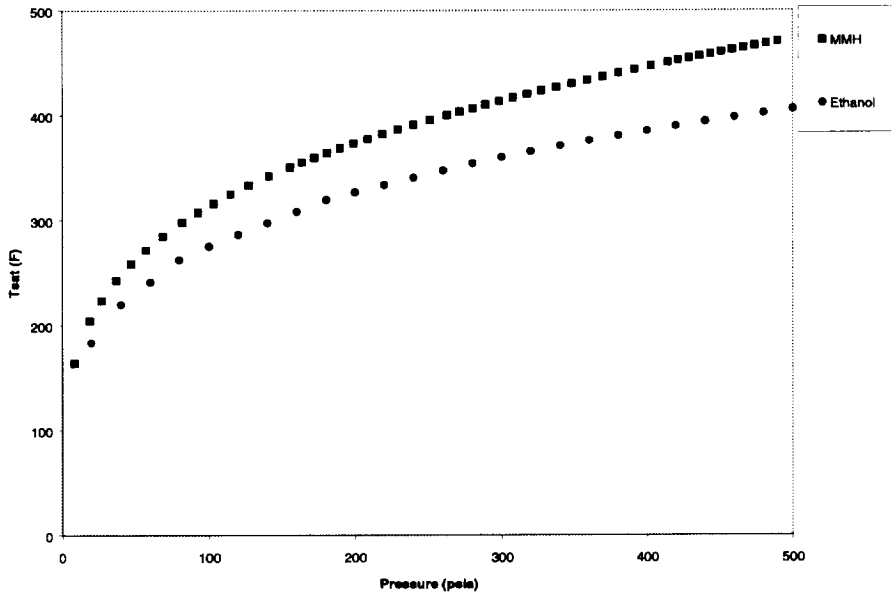

Figure 3. Propellant Saturation Temperature

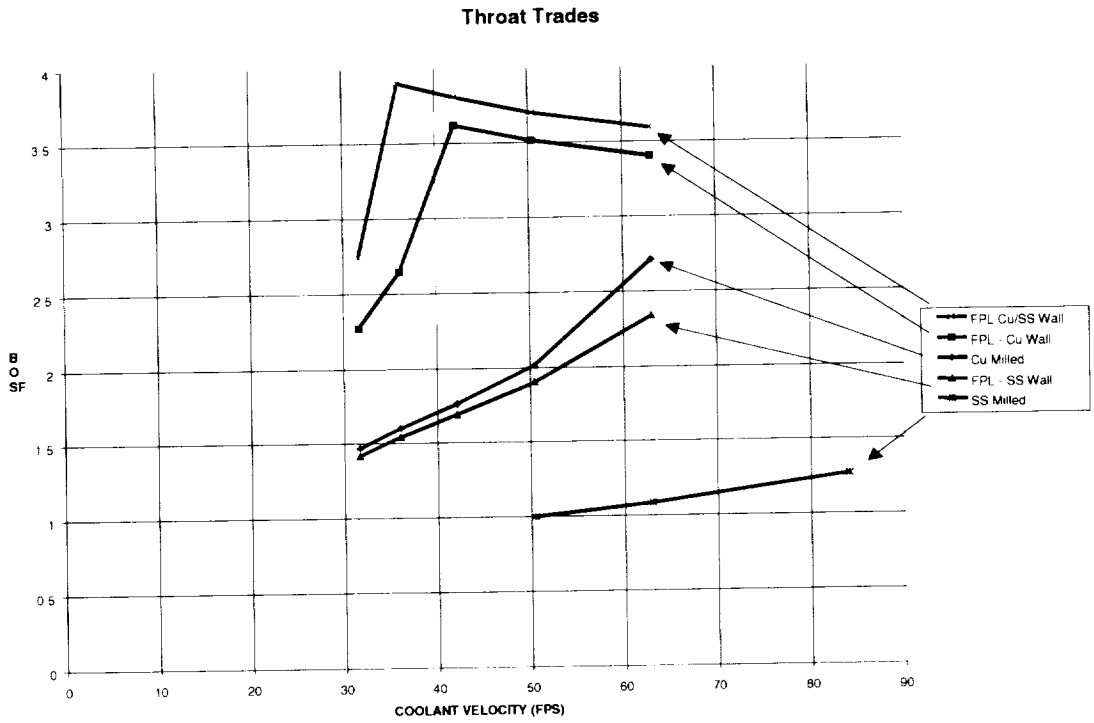

Figure 4. Throat Region BOSF

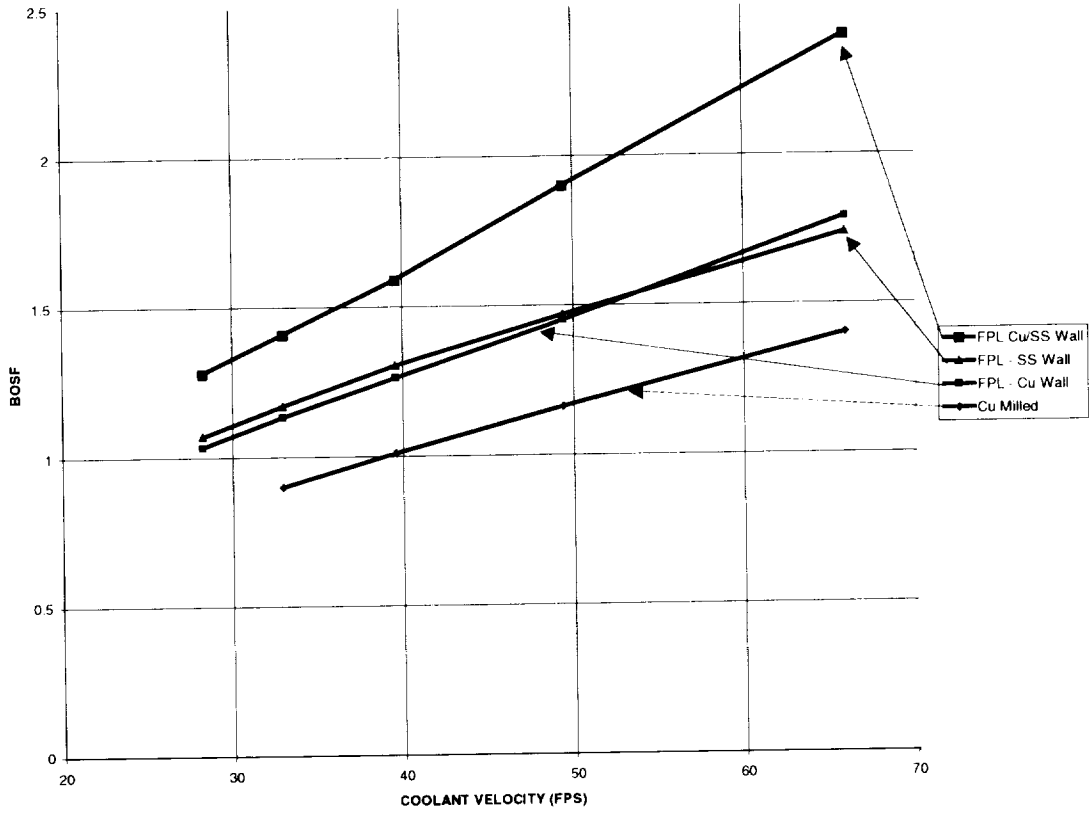

Figure 5. Barrel Region BOSF

3.0 Fabrication Demonstration

3.1 Demonstration Description

The thermal analysis and trade studies, as discussed in section 2.0 of this report, identified the most the most thermally efficient design concept to have a composite hot gas wall made up of .020" stainless steel backed by .020" copper. Such a design is not readily obtainable by conventional fabrication techniques. However, this configuration was thought to be readily producible by Aerojet's platelet technology. A demonstration of the composite stainless and copper hot gas wall in formed platelet liner panels was therefore planned.

In order to reduce costs, available formed platelet tooling residual to previous programs, was examined for applicability to a demonstration non toxic formed platelet liner panel. It was determined that the original 40k tooling fabricated under NASA contract NAS 8-37456, was of a size appropriate to approximate the non-tox conceptual design. This tooling was being surplused by the NASA contract and was therefore available to be purchased by the non-toxic program. A comparison of pertinent features of the Non-Toxic OMS-E flight-type conceptual design and the demonstration panel design features are shown in Table 2.

	Conceptual Design Non-Toxic OMS-E FPL	Demo Non-Toxic "40k" FPL
Barrel Dia (in)	7.0	5.66
Throat Dia (in)	4.8	3.31
L' (in)	16.0	4.9
Liner thickness, t (in)	0.140	0.140*
Upstream Radii, R1 R2 (in)	2.4	1.655
Downstream Radius, R3 (in)	2.4	1.655
t/R_{min}	.058	.085

* Original hotfired 40k liner thickness was .255 inches. Shims were used to reduce functional panel thickness to Non-Tox OMS design thickness

Table 2. FPL Design Parameter Comparison

Although the 40k design is nominally smaller than the Non-Toxic OMS-E concept, the critical formed platelet liner parameter of minimum bend radii (usually the downstream, divergent or R3 radius) divided by liner thickness are similar. In fact, the resultant demonstration panel ratio is greater; this results in these panels being slightly more difficult to form than the Non-Toxic OMS-E conceptual design. Figure 6 provides a graphical explanation of the forming parameter and also displays Aerojet's FPL experience. As can be seen in the figure, where the liner thickness / R3 ratio is plotted vs. throat radius, the demonstration panels provide a worst

provide a worst case design. The thinking here was if the composite hot gas wall could be successfully formed at the 40k size, then the conceptual flight type design would be readily formable.

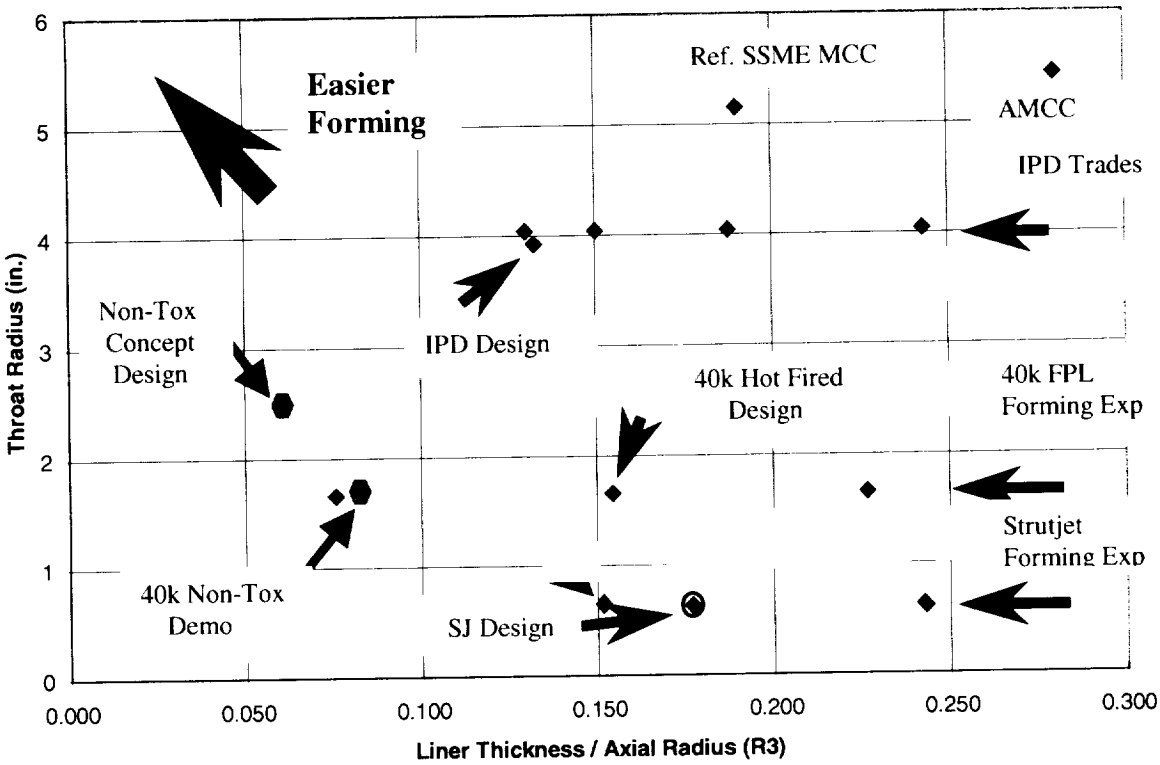

Figure 6. FPL Forming Experience

After the decision made to utilize the 40k tooling for the demonstration panels the next decision to be made was platelet / panel layout. It was determined that the basic 40k platelet layout would be satisfactory for the demonstration panels. The basic difference was that the lands and channels in the 40k design would be slightly (~.005") smaller than the conceptual design. Again, the logic was that the 40k design offered a higher degree of difficulty in forming than an actual Non-Toxic OMS-E FPL of the current conceptual design.

In order to demonstrate the proper panel thickness, which was considered to be pertinent to the concept demonstration, a novel approach was adopted. As the 40k forming tooling has a set gap of approximately .250" and the desired Non-Toxic demonstration panels had a thickness of .140", formed platelet shims were used to accommodate the reduced thickness. These shims were built integral with the platelet stacks at the time of assembly and were separated from the functional panels by a layer of stop-off. After forming the "shim" was removed, leaving the desired thickness panel.

Per the thermal trade studies, the hot gas wall of the demonstration panels was to be a composite, or bi-metallic, wall consisting of .020" of stainless steel and .020" of copper. 347

because of their strength at elevated temperature and previous platelet experience and application. The lands of the channels were also identified as copper through the thermal studies; again ZrCu was chosen for this area.

Included in the conceptual Non-Toxic OMS-E design is the novel idea of an integral structural jacket. The manner in which this achieved is to use a high strength material for the final closeout platelet in the panel. Following forming, during the weld assembly of the individual panels, the edges of the high strength sheets are joined together resulting in the formation of a structural can or jacket around the liner. This manner of producing the required structural load carrying capability for a combustion chamber appears particularly well suited to relatively low chamber pressure applications as in this pressure fed OMS-engine.

In previous designs, electroformed nickel or welded corset type structures have been used to provide the required structural jacketing. This new integral jacket approach promises to offer significant cost, potential weight and significant fabrication time reductions over its predecessors.

For the purposes of the demonstration panels fabricated, two configurations of panel were chosen. To demonstrate the integral structural jacket, one of the configurations had a .020 stainless steel platelet closeout. As the integral structural jacket approach was new and untried, the second configuration panels had standard ZrCu closeouts.

Due to availability, and its weldability over 347CRES, 304l CRES was chosen as the material for the closeout platelet in the integral jacket panel configuration. Subsequent hand calculations showed for 304l the closeout should have been approximately .042" thick; for a Nitronic40 class material, .040" thick, and for a .02" closeout, an A286 class material would be required. These hand calculations used the strength of the existing electroformed OMS-E jacket as a basis for comparison. Actual closeout sizing would require higher fidelity modeling and analysis. It should be noted that a higher strength or thicker closeout would add forming difficulty and needs to be further investigated.

A flowchart depicting the fabrication and evaluation plan for the demonstration panels is shown in Figure 7. Eight panels were fabricated, four of each of the two configurations described above. Figure 8 shows a loose stack of typical platelets that went into the assemblies. Figure 9 shows the cold forming operation, including a flat bonded panel and an as formed panel with the forming frame still attached.

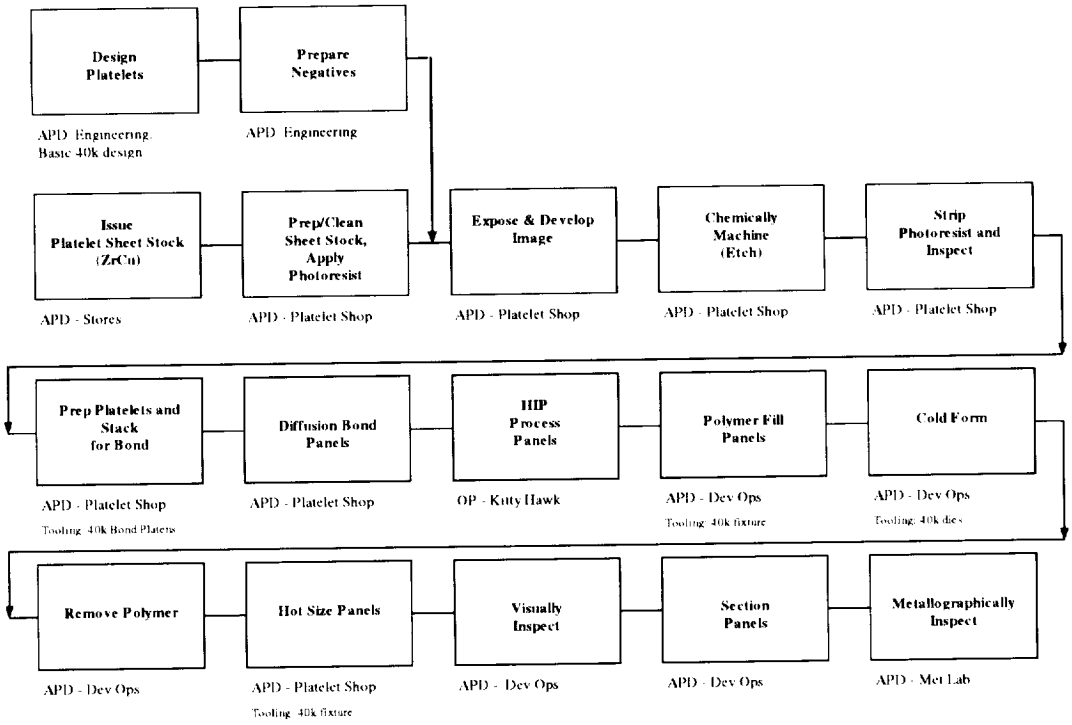

Figure 7. Demonstration Panel Fab Plan

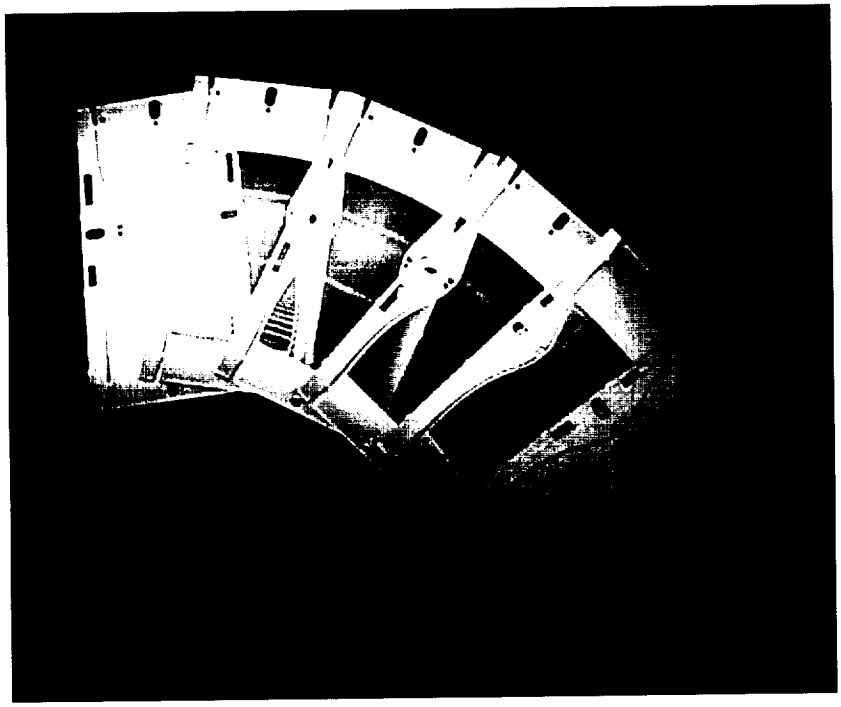

Figure 8. Typical Non-Toxic OMS-E Demonstration Panel Platelets

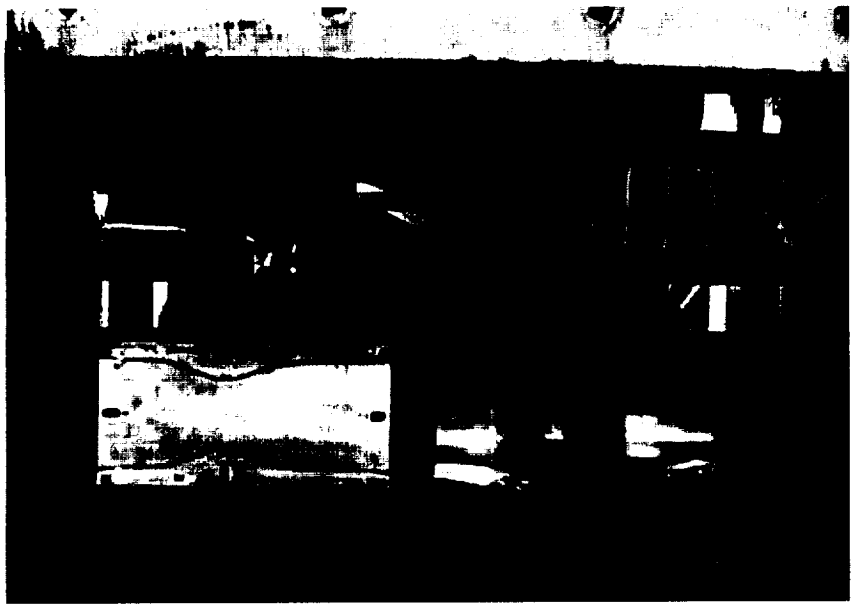

Figure 9. Demonstration Panel Cold Forming

3.2 Demonstration Evaluation Results

Visual examination of the panels following cold forming proved exceedingly encouraging. No visible wall damage or channel collapse was apparent. This was the case for both configurations of panels formed, the conventional copper closed out panels and those closed out with stainless steel. The panels looked exceptionally well, even for a first attempt at the new composite hot gas wall configuration.

The evaluation of the demonstration panels included a water cold flow following the forming operations. Figure 10 shows the low flow pattern check of one of the formed panels. Highly uniform flow is apparent. A comparison of the cold flow data obtained from four of the panels is included in Figure 11. The data groups exceptionally well, indicating a high degree of repeatability in the process.

Following cold flow, the panels were sectioned and prepared for metallurgical examination. Figure 12 shows the manner in which the panels were sectioned. Figures 13 and 14 show typical cross sections of a stainless steel and a ZrCu closed out panel, respectively. Both sections show good channel and land uniformity.

The sectioned panels underwent metallurgical examination. A typical photomicrograph of the stainless steel to ZrCu diffusion bond is shown in Figure 15.
The bond quality is considered excellent. No voids, inclusions or other abnormalities are evident.

Figure 10. Low Flow Pattern Check of Demo Panel

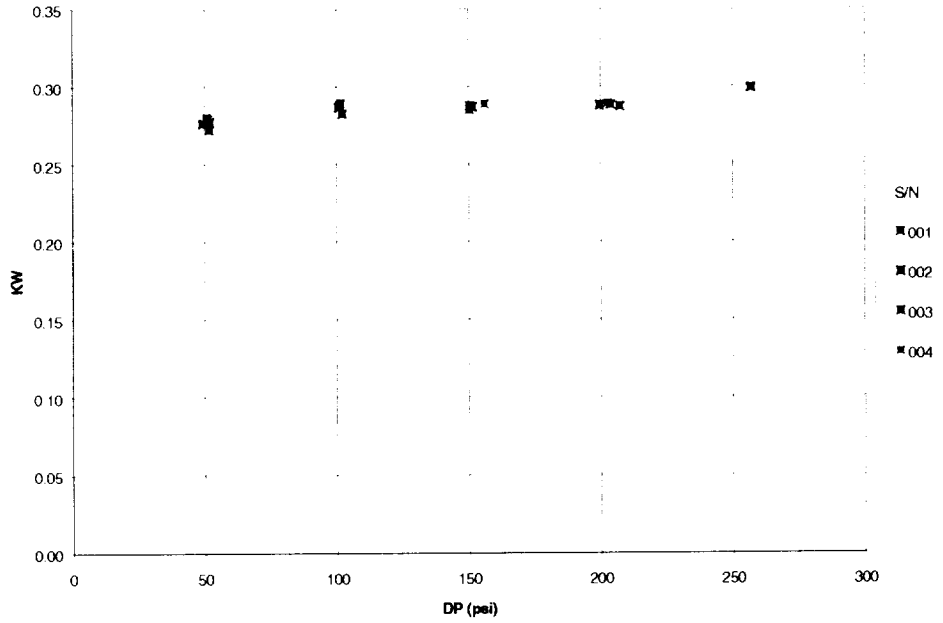

Figure 11. Demo Panel Cold Flow Results

Figure 12. Sectioned Non-Toxic Demonstration Panel

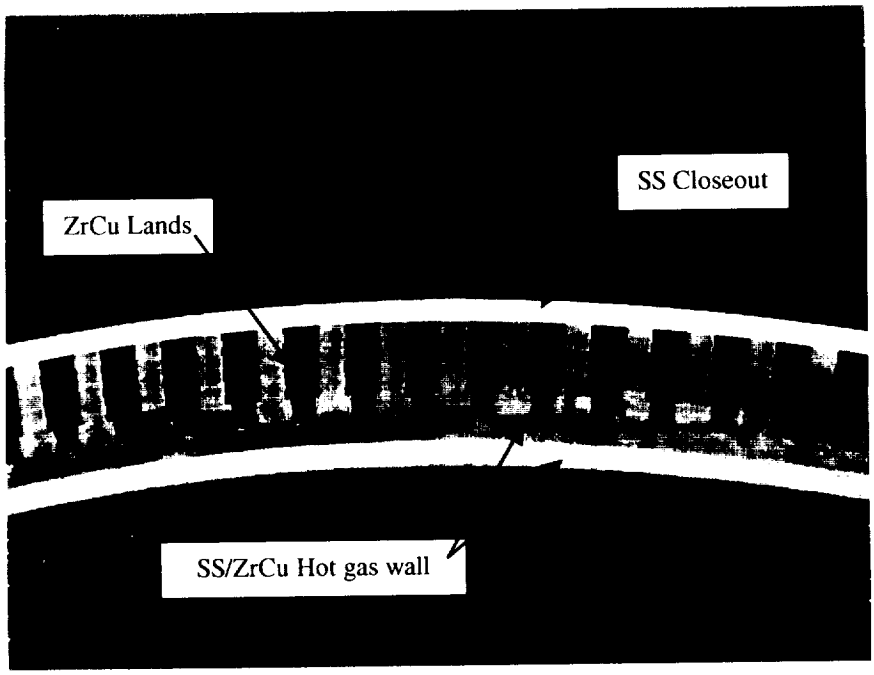

Figure 13. Sectioned Demo Panel w/ SS Closeout

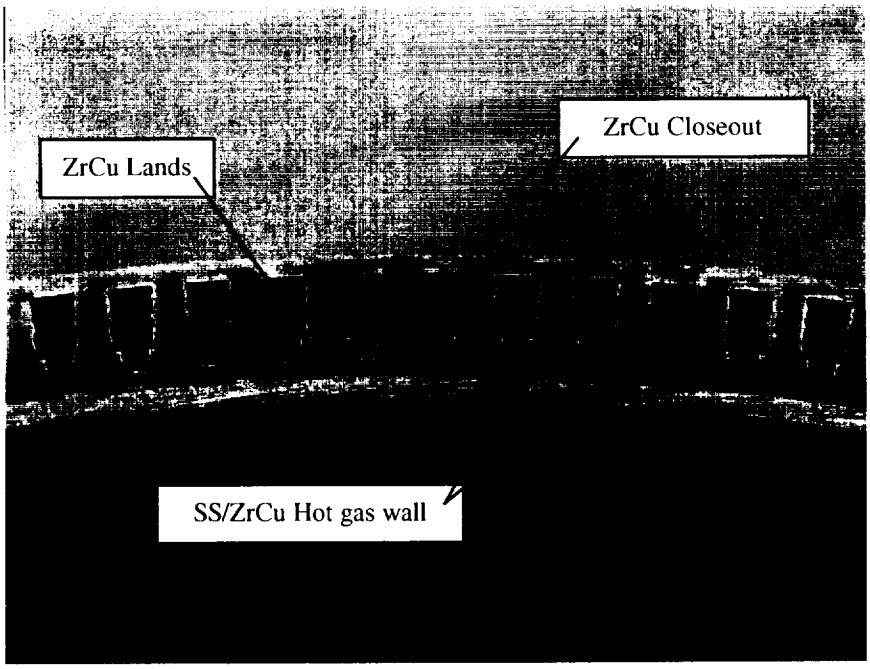

Figure 14. Sectioned Demo Panel w/ Cu Closeout

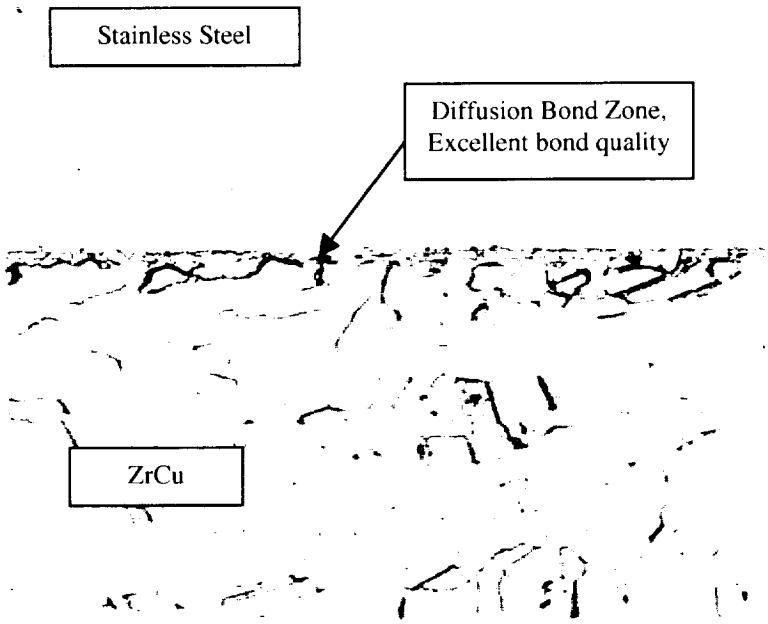

Figure 15. Stainless Steel to ZrCu Diffusion Bond

3.3 Fabrication Demonstration Conclusions

All of the results obtained from evaluations of the demonstration panels proved to be positive. None of the evaluations performed identified issues of concern. From a fabricability standpoint, this shows the concept of a formed platelet liner employing a composite stainless steel and copper hot gas wall to be valid. Further, the successful fabrication of panels with stainless steel closeouts supports the concept of a formed platelet liner with an integral structural jacket.

4.0 Material Properties Testing

4.1 Introduction

In addition to channel burnout described previously under the thermal design section of this report, coolant channel hot gas wall low cycle fatigue is also a potential failure mode of regeneratively cooled combustion chambers. Although Aerojet has significant experience with bi-metallic diffusion bonds of the type employed in this chamber concept, we had no data on the low cycle fatigue characteristics of this combination. In order to obtain relevant data for such an application, a materials test program was instituted.

The results of the testing and subsequent analysis showed cycle life in excess of the 1000 hot fire cycle requirement to be readily achievable with this combination of materials in this application.

4.2 Test Specimen Description

Tensile and low cycle fatigue (LCF) tests were performed on a 3 x 3 x 3.5" diffusion bonded block, consisting of alternating 0.020" Cres 347 and zirconium-copper (ZrCu) platelets. The diffusion bonded block was processed in accordance with parameters defined for the actual part, including a HIP at 1100°F by Kitty Hawk (Garden Grove, CA). All machining and testing was performed by Metcut Research Associates, Inc. (Cincinnati, OH). Cylindrical specimens were sectioned from the block, perpendicular to the bond planes. Reduced gage section tensile and fatigue specimens were machined to the configurations shown in Figs. 16 and 17 respectively. Four tensile specimens were tested at room temperature and four were tested at 400°F. Six fatigue specimens were tested under constant amplitude strain control, three at room temperature and three at 400°F. LCF testing was performed at three different total strain ranges, for a strain ratio R = 0.1. Strain ranges were selected initially from analytical results obtained from previously designed formed platelet chambers, all of which were cooled with cryogenic hydrogen.

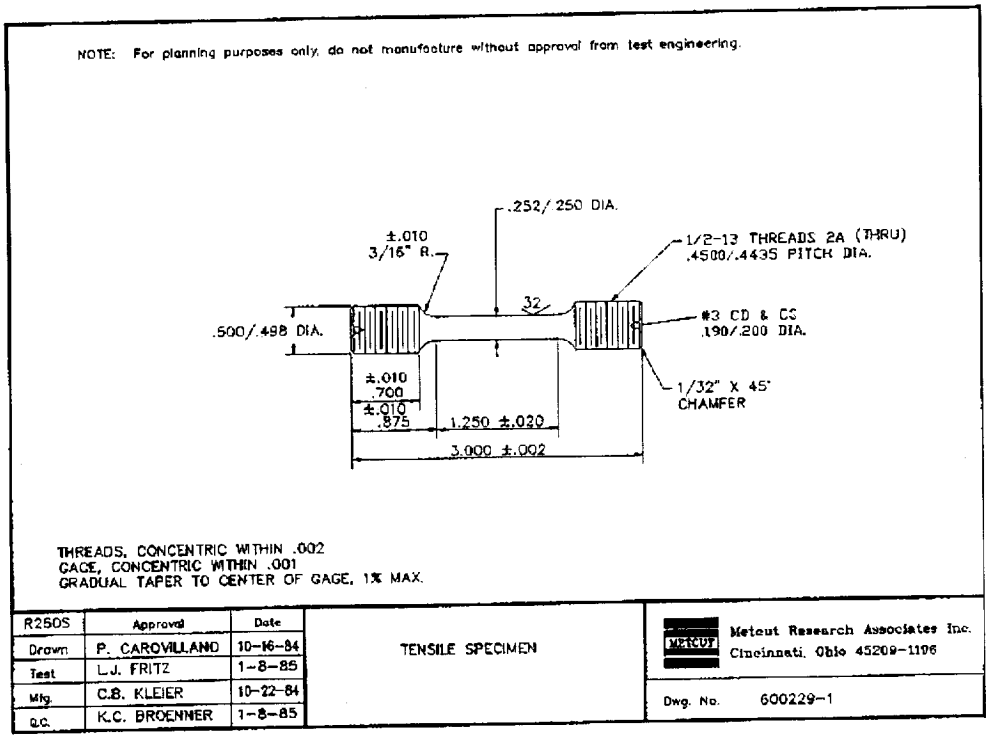

Figure 16. Tensile specimen configuration.

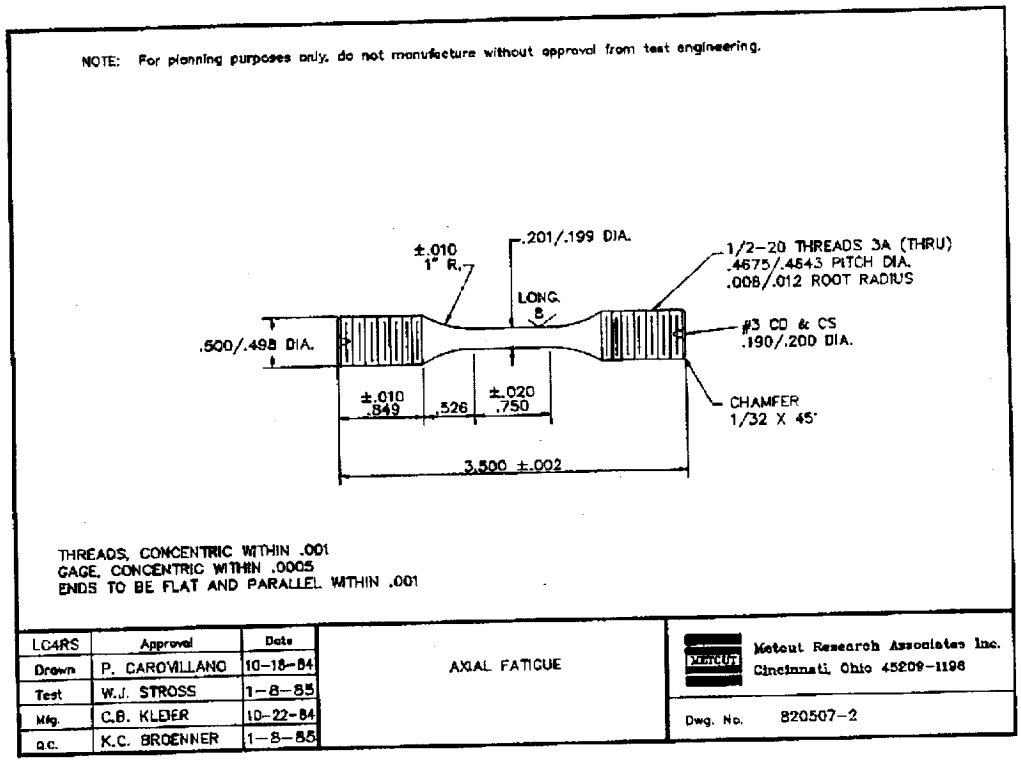

Figure 17. Low cycle fatigue specimen configuration.

4.2 Testing Results and Discussion

Tensile test results are presented in Table 3. Ultimate strength is significantly higher than that reported for diffusion bonded ZrCu alone. Artificial strengthening may be a result of the specimen configuration with thin layers of alternating materials. Although values for 0.2% offset yield strength, elongation and reduction in area are reported, the significance of these values for comparison with ZrCu is minimal due to a non-uniform gage section (having two materials with significantly different elastic properties.

LCF test results are presented in Table 4. Initially, it appeared that specimens had failed at significantly lower numbers of cycles as compared to diffusion bonded ZrCu alone, tested under similar test conditions. The fracture surfaces were predominantly flat in appearance and consistently occurred near the interface between the copper and stainless steel. It was hypothesized that either the apparently premature failure resulted from a bonding process issue, or that the failure was not premature at all, but rather a result of high localized strains resulting from the specimen configuration with the thin layers of two elastically different materials.

To test the first hypothesis, analyses were performed on the fracture surface of a typical LCF specimen. Analyses included visual examination, a surface analysis by electron microprobe (EMP), and a scanning electron microscope (SEM) evaluation. Visual examination of the fracture surface indicated the majority of the failure occurred within or at the Ni strike. The EMP analysis indicated no detrimental contaminants at the fracture surface. The SEM examination of the fracture surface indicated that there were no areas of incomplete bonding. The entire surface was composed of fatigue striations, shear-lips, and dimples (Figs. 4 and 5), typical of a fatigue failure. Based on the results of these analyses, it was concluded that the apparently reduced fatigue life was not a result of a bonding process issue.

Spec ID	Temp (°F)	UTS (ksi)	0.2%YS (ksi)	Elong (%)	RA (%)
1	75	58.0	24.2	32.0	43.0
2-RM	75	57.0	25.6	23.0	28.0
3	75	58.5	24.1	31.0	36.0
4	400	43.4	20.0	25.0	39.0
5	400	42.3	20.0	20.0	35.0
6	400	43.4	19.0	19.0	34.0

Table 3. Tensile Test Results for Diffusion Bonded SS/ZrCu Materials

Spec ID	Temp (°F)	Unadjusted TSR* (%)	Adjusted TSR* (%)	Nf (cycles)
7	75	0.4	1.079	6568
11	75	0.6	1.584	1993
8	75	0.8	2.084	1545
10	400	0.4	0.97	7903
12	400	0.6	1.463	4121
9	400	0.8	1.922	3983

* Unadjusted TSR values represent overall strain in gage section.
Adjusted TSR values represent predicted local maximum strain ranges.

Table 4. Low Cycle Fatigue Test Results for Diffusion Bonded SS/ZrCu Materials

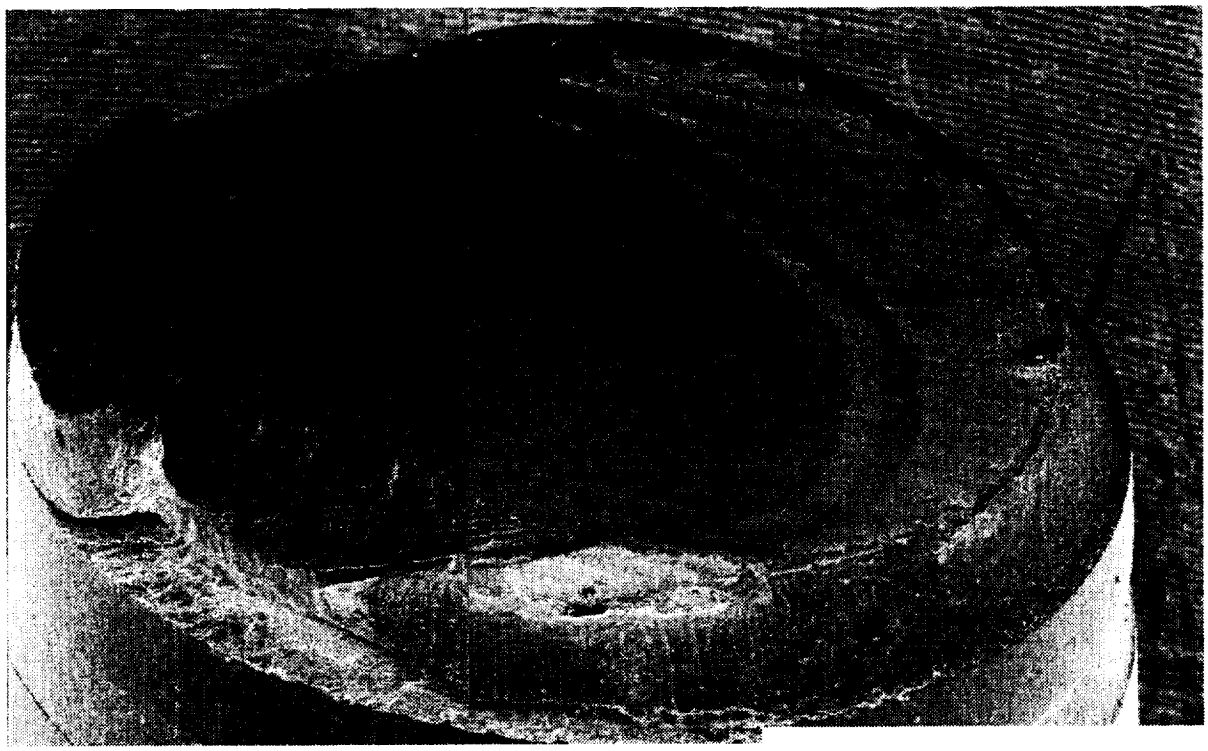

Figure 18. Secondary electron image of fracture surface from a typical LCF specimen.

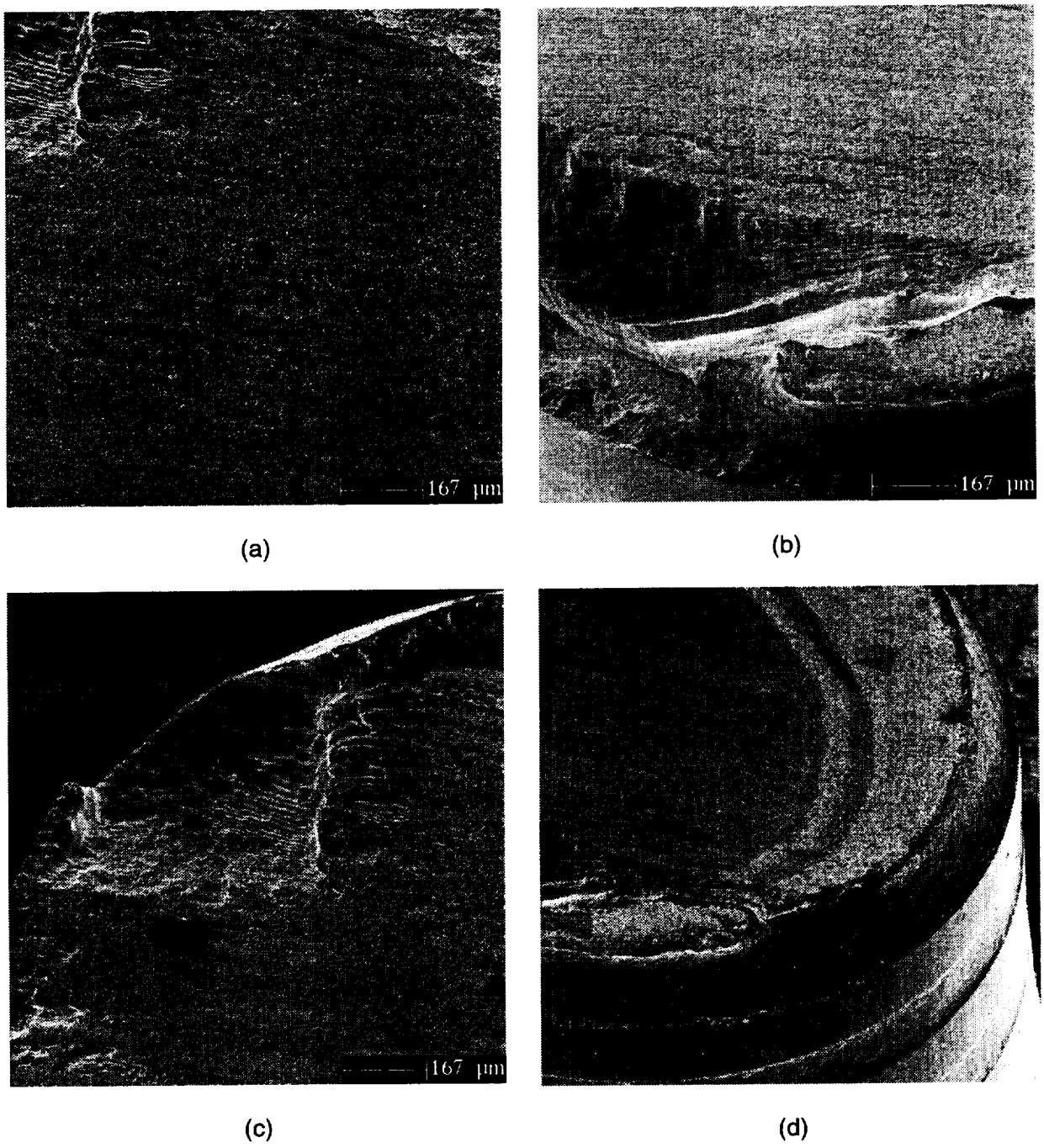

Figure 19. Secondary electron images from fracture surface in Fig. 4, at higher magnification show areas from the center, and edges. The center area (a) exhibited dimpling, and at the edges (b,c) were fatigue striations and (d) a shear-lip region.

To address the second hypothesis, that of high localized strains resulting from the specimen configuration, finite element modeling (FEM) of the specimens tested was performed. In addition, to validate the assumed strain range used for testing, a finite element model of a cross section of a throat area channel / land combination was also constructed.

Figures 20 and 21 show the LCF specimen FEM strain plots at 70 degrees F and 400 degrees F, respectively, for .4% total strain. Similar analysis was performed for .6 and .8% total strain. Figures 22 , 23 and 24 show the thermal plot, strain plot and VonMises stress plot, respectively, for the channel / land model.

The results of the structural analysis on the fatigue specimen and a throat cross section for the Non-Toxic OMS-E configuration yielded two significant conclusions. First, the finite element model of the fatigue specimen indicates that the actual strain in the specimen was much higher than the strain that was assumed input based on deflection of the gage length. There is a significant increase in strain developed in the ZrCu, at the interface with the stainless steel as shown in Figures 21 and 22. The cycles to failure, and these actual (calculated maximum) strains, have been used to produce fatigue curves at 70 and 400 F, as shown in Figure 25. The data in also shown tabulated in Table 4. Both the graphical plot and the table show unadjusted and adjusted strain ranges that represent, respectively, the test cross head movement total strain and the FEM calculated total strain.

In Figure 25, the developed 400 F curve correlates well with existing fatigue data for ZrCu platelet structures obtained during the AMCC formed platelet liner program. The corresponding 70 F curve however shows lower than expected fatigue life. It is felt that the specimen configuration (SS/ZrCu/SS/.....) potentially introduced work hardening of the ZrCU. This work hardening would be sufficient to cause the lower than expected fatigue life witnessed. At elevated temperatures representative of the operational temperature this does not appear to be an issue, as evidenced by the 400 F curve and from review of existing data on work hardening of ZrCu at various temperatures. Fortunately, no yielding occurs in the ZrCu at 70 F for this design, therefore the lower than expected data is not of concern.

The second significant conclusion was reached following completion of the finite element model created of a typical channel and land configuration in the throat. This model was run for pressure and thermal loading. The results indicate that the maximum strain is developed entirely in the stainless steel platelet on the hot gas wall. The bond interface between the stainless steel and the ZrCu does not yield and therefore should not limit fatigue life. Because the strain is entirely concentrated in the stainless steel platelet at the hot gas wall, fatigue curves for CRES 347 were used at 800F and a 10 minute hold time. The resulting fatigue life estimate for this formed platelet OMS engine, based on the typically life limiting throat area analysis, is 1750 cycles using a safety factor of 4 on cycles. This estimate, which is significantly higher than the 1000 cycle requirement, shows the robustness of the formed platelet composite hot gas wall design.

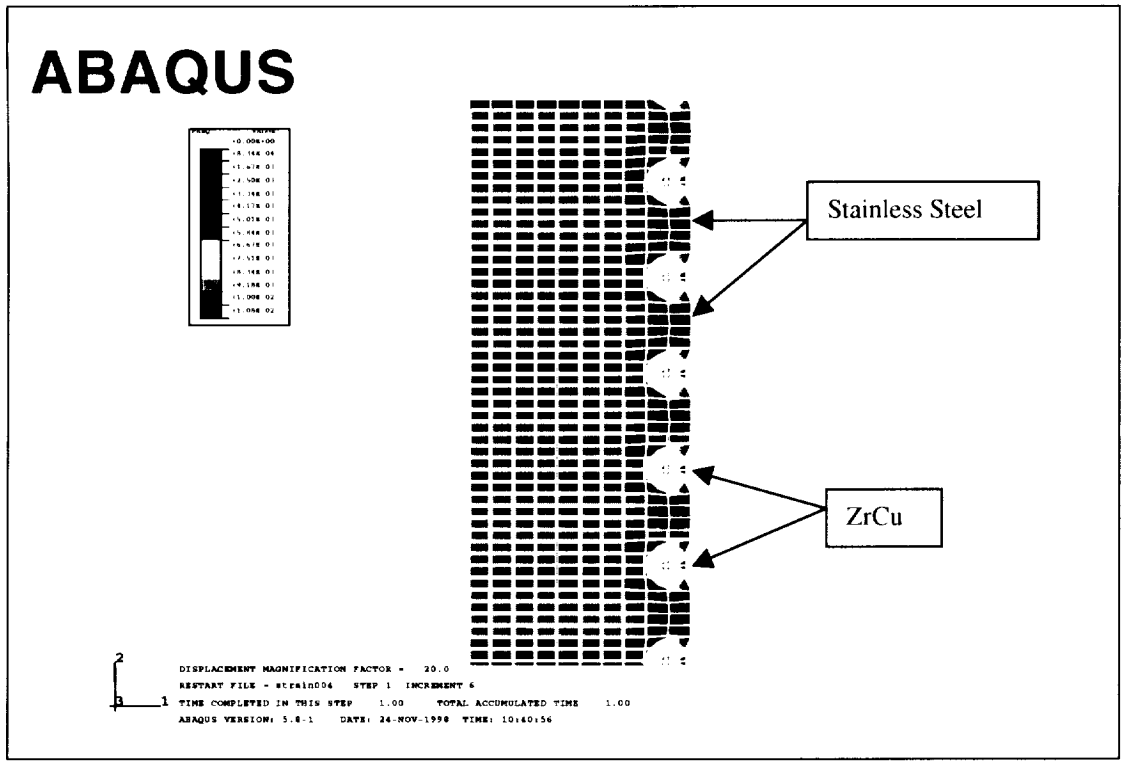

Figure 20. .4% Total Strain, 70F – Strain Results

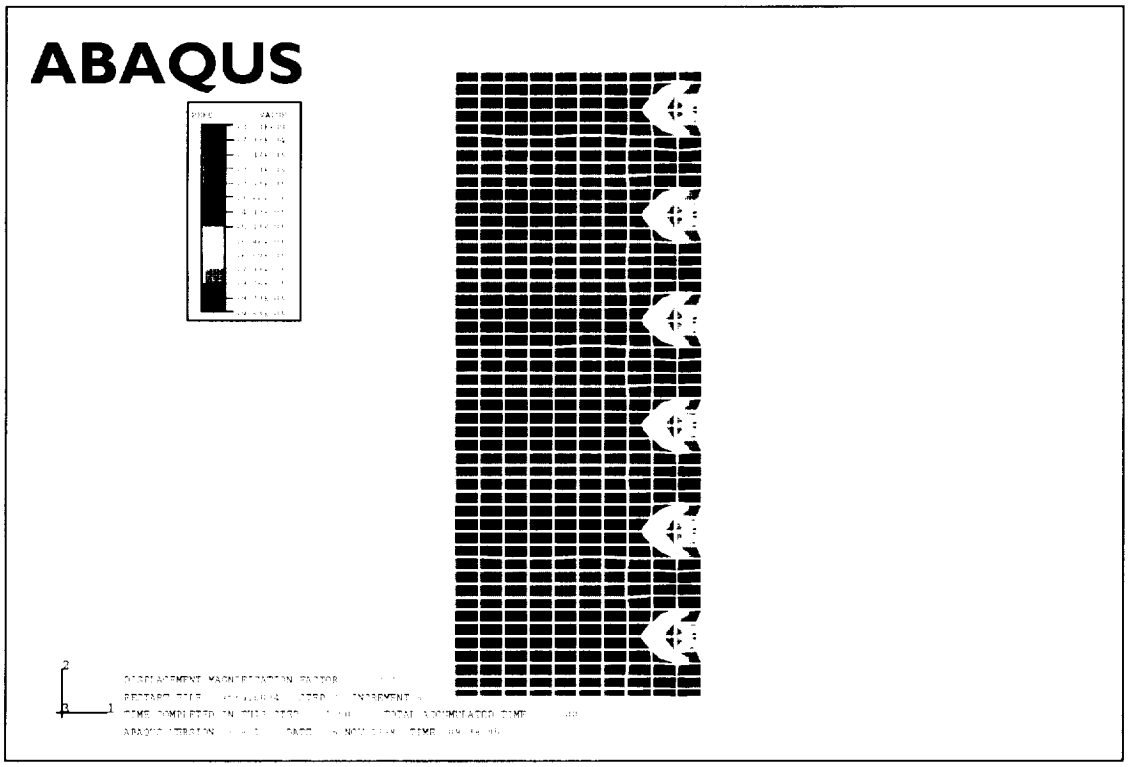

Figure 21. .4% Total Strain, 400F – Strain Results

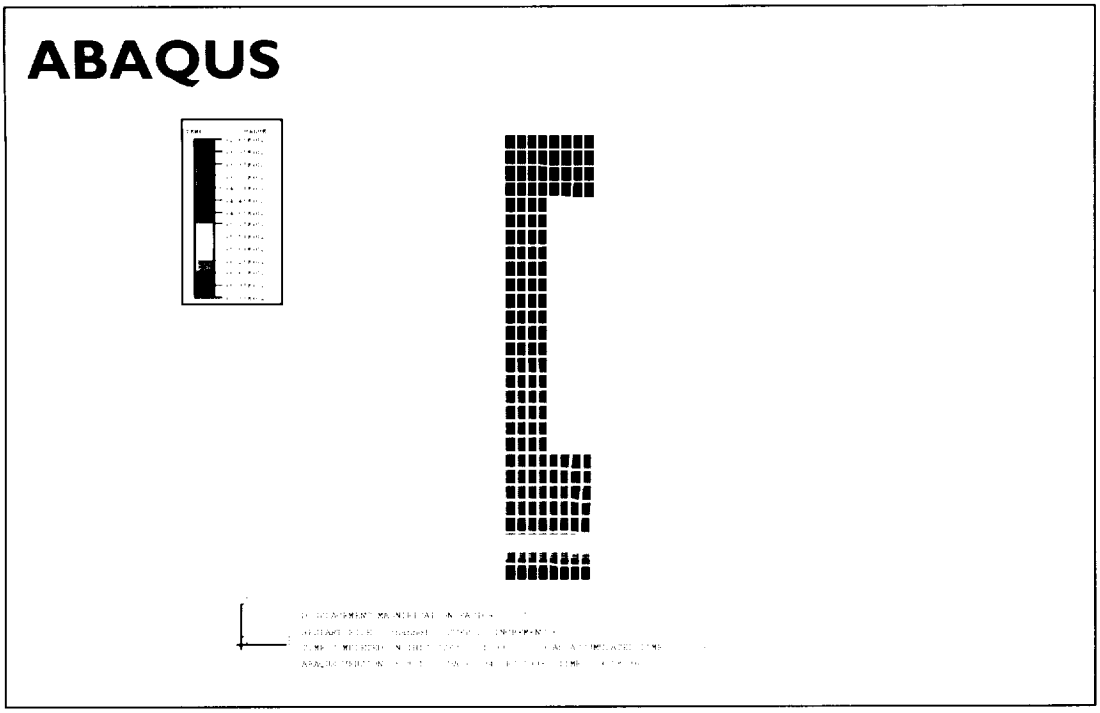

Figure 22. Throat Area – Thermal Plot

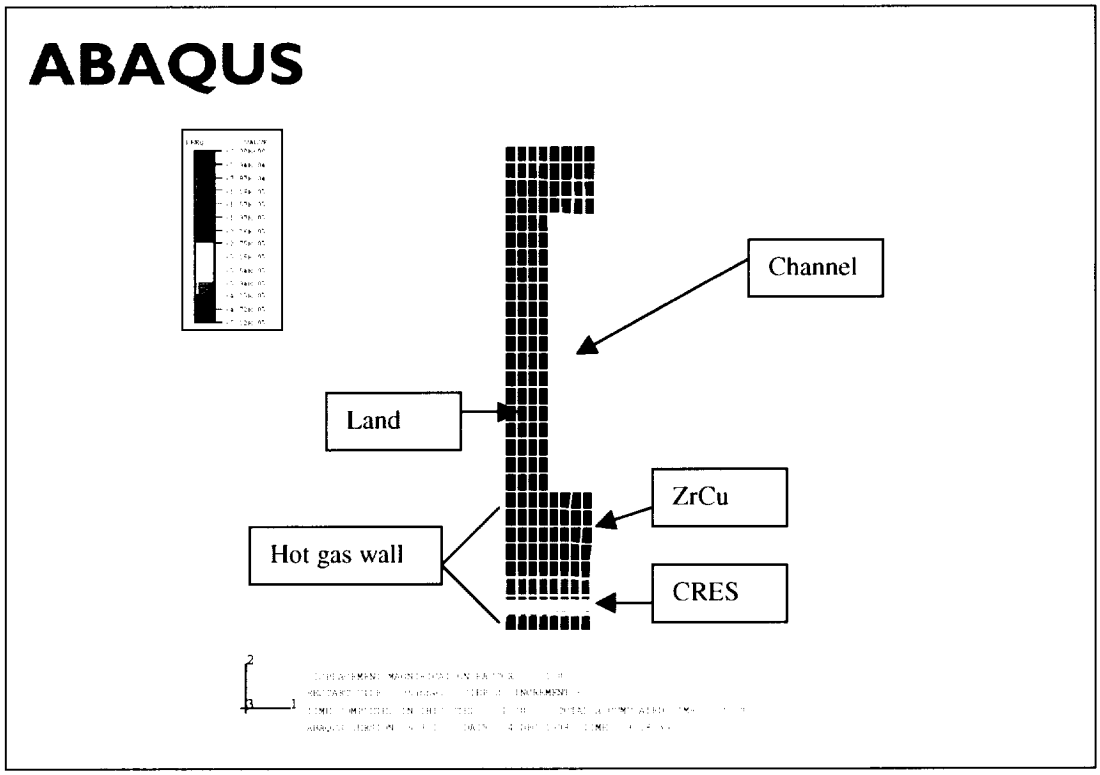

Figure 23. Throat Area - Strains

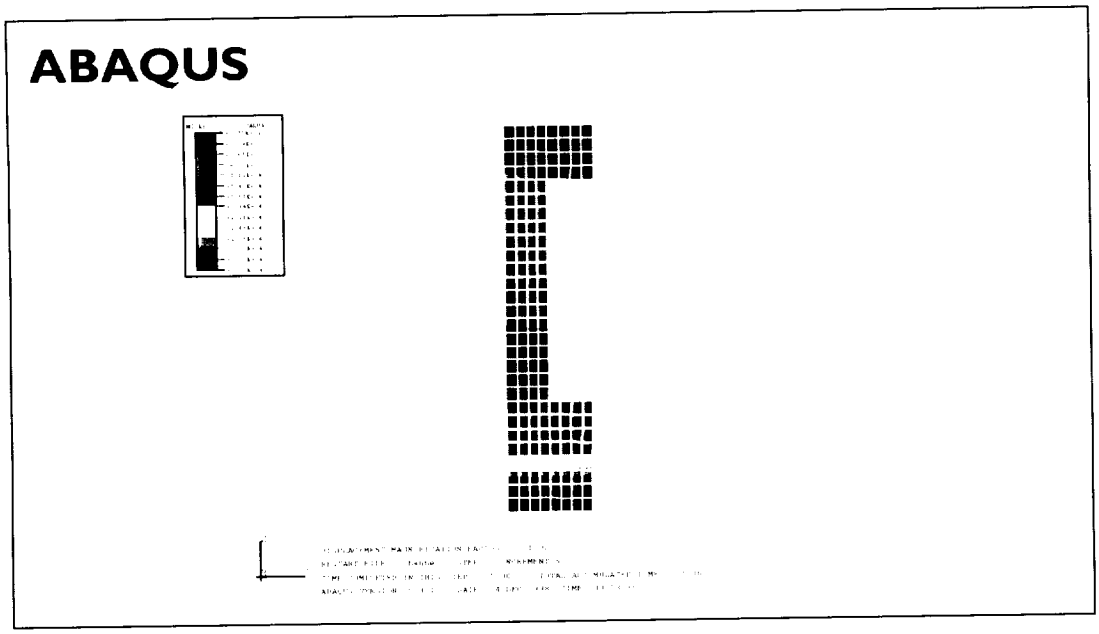

Figure 24. Throat Area – Von Mises Stresses

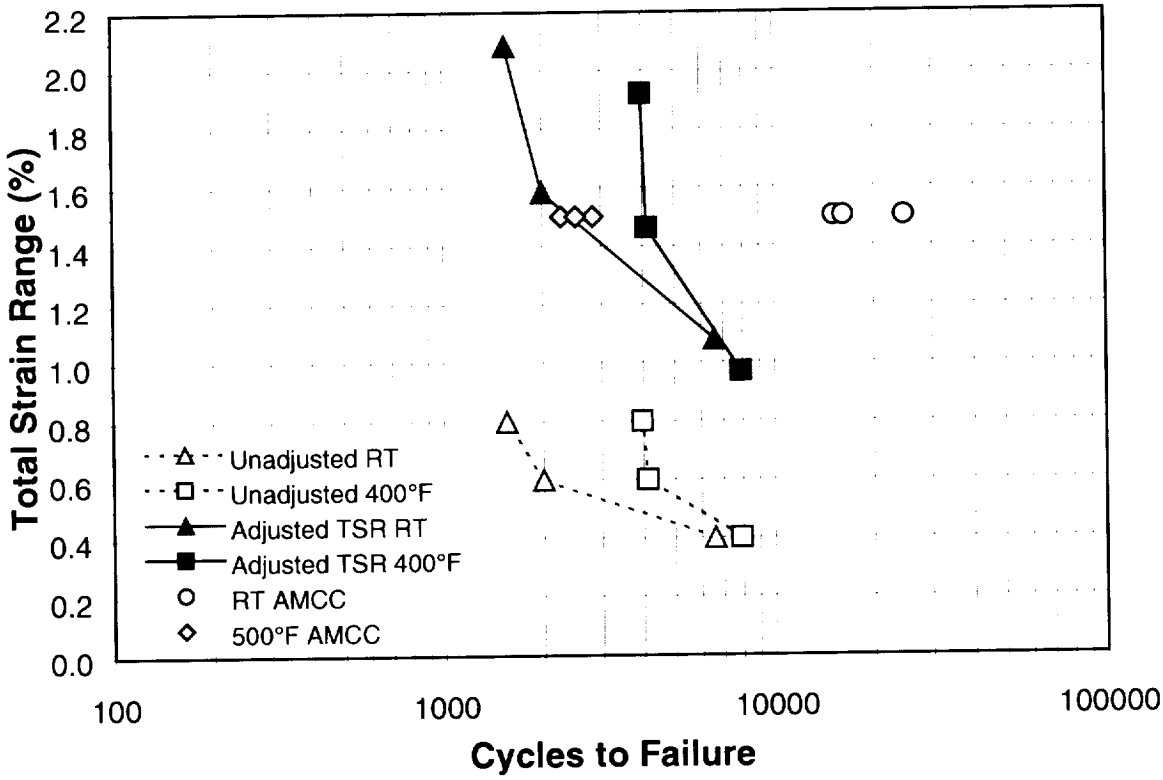

Figure 25. Low cycle fatigue results for SS/ZrCu diffusion bonded block as compared to data for diffusion bonded ZrCu on AMCC program. Data are plotted with adjusted and unadjusted total strain range (TSR) values.

5.0 Conclusion and Recommendations

This program investigated the use of ethanol as a coolant for a replacement combustion chamber for the Space Shuttle Orbiter OMS engine. Analytical trade studies performed identified a composite hot gas wall employing stainless steel backed by copper as the most thermally efficient option. Formed platelet liner panels with this configuration hot gas wall were fabricated and evaluated. Panels employing a stainless steel closeout to form an integral structural jacket were also fabricated and evaluated. Mechanical properties specimens of the noted composite construction were prepared and tested.

The results of the trade studies provided the basis for a concept for a flight type chamber with a formed platelet liner. This concept was modeled and utilized other new low cost components, including a flight type injector scaled from a 1998 Aerojet IR&D program and low cost cast manifolds.

Evaluation of the formed platelet liner panels fabricated to demonstrate the hot gas wall concept showed positive results. These evaluations included visual inspection, cold flow, destructive sectioning and metallographical examination. The panels containing the stainless steel closeout forming the integral structural jacket, also showed positive results during evaluation. This integral jacket approach promises to reduce fabrication costs and lead times.

Testing and analytical evaluation of the mechanical properties specimens showed low cycle fatigue life consistent with diffusion bonded ZrCu, the common material of construction for a formed platelet liner. Analysis also showed, for this design, that yielding does not occur in the bond zone between the stainless steel and copper. Yielding was predicted to occur only in the stainless steel portion of the hot gas wall.

Combining the analytical results of the trade studies and the mechanical properties testing and evaluation provides a predicted life of >1700 hot fire cycles with a burnout safety factor of 1.5. Such a design would more than meet the current OMS requirement of 1000 cycles.

It is concluded that a long life, optimized design combustion chamber for a Non-Toxic Space Shuttle Orbiter OMS engine is achievable. Further it is concluded that such a design is best fabricated using the formed platelet liner approach which brings with it inherent low cost and short fabrication spans.

It is recommended that further consideration of this approach be given. A demonstration engine could be fabricated utilizing available tooling and scaleable injector designs. Alternately, investment in new chamber tooling would result in a demonstration engine of an optimized size for the Space Shuttle Orbiter OMS application.

APPENDIX A

References

1. Rousar, D., Young, M., Ferrante, F., and Greisen, D. " A Proven Approach for Correlating the Critical Heat Flux of Coolants ", 49th International Astronautical Congress, September 28-October 2,1998, IAF-98-S.3.02

2. Meyer,M.L.,Linne,D.L., and Rousar,D.C., " Forced Convection Boiling and Critical Heat Flux of Ethanol in Electrically Heated Tube Tests", AIAA-98-1055, 36th Aerospace Sciences Meeting and Exhibit, January 12-15, 1998 Reno, Nevada

3. Elam,S.K., Hayes,W.A., "Subscale Hot-Fire Testing of a Formed Platlet Liner", AIAA/SAE/ASME/ ASEE 28th Joint Propulsion Conference and Exhibit, June 28-30 1993, AIAA-93-1827

APPENDIX B

Platelet Device Design and Fabrication

Since 1964 Aerojet has been developing and utilizing Platelet Technology to provide solutions to difficult thermal and fluid flow problems in a wide variety of applications. In this Aerojet-unique technology, through and/or partial depth etched patterns are chemically machined with photographic accuracy in thin sheets of metal, or platelets. Figure B1 displays the manner in which this chemical machining is performed. Following chemical machining these individual platelets are in turn accurately stacked and diffusion bonded together to form essentially monolithic structures having internal passages. These passages can contain precise fluid metering orifices and in-situ filters. In variations of the process, the bonded assemblies are machined or formed into finished products or components of other devices. Figure B2 displays the manner in which individual platelets are stacked to form an assembly.

The platelet process lends itself to mass production via its basic reliance on the well established process of photo-chemical machining, a process widely used in the printed and integrated circuit industries. The diffusion bond assembly process has been extensively studied, developed and utilized at Aerojet over the past 35 years.

Metals regularly used in the platelet device manufacturing process include stainless steels; copper, nickel, aluminum, titanium and their alloys; additionally work has been performed with high strength, high temperature and exotic materials. Composite or bi-metalic structures are also quite common.

Traditional devices designed and constructed utilizing Platelet Technology include liquid rocket engine propellant injectors, cooled combustion chambers and nozzle extensions, transpiration cooled devices such as re-entry vehicle nosetips, IR windows, radomes, and leading edges. Recently, Aerojet has applied Platelet Technology to other applications for heat transfer and fluid flow control devices such as heat pipe wicks, heat exchangers, fuel cell separators, and electronic chip coolers. Figure B3 displays a variety of platelet devices.

The basic platelet device design and fabrication process is outlined in Figure B4. Seen in the first picture is the design originating on our CAD system. The design files are then transferred to our photo-tooling department, shown in the second and third pictures, where they are converted into the files to drive our Laser photoplotter. The photoplotter produces negative image masks, plotted on mylar.

Sheet stock to be used to fabricate platelets is shown being cleaned and prepared for etching in the forth picture. The fifth frame shows the two sided application of a light sensitive material known as photoresist. Shown next is the image transfer or exposure, where the photoplotted negative image masks are used to transfer the an image onto the light sensitive photoresist in a contact printing operation. Not shown is the developing operation where photoresist that was masked from the exposure light is washed away to reveal the bare sheet stock surface.

Chemical machining, or etching is shown in the next frame. In this operation, the areas of the sheet stock not covered with the photoresist material are chemically attacked by chemical solutions referred to as etchants. Following removal of the photoresist material by additional chemical processes not shown, the completed platelets are inspected on computerized non-contact coordinate measuring machines. This operation is shown in the ninth frame.

After acceptance through the inspection process, individual platelets are prepared for diffusion bonding by chemical cleaning of the surfaces and generally application of a suitable bond aid. This bond aid is usually electroplated on the surface. Inspection of the bond aid is made by x-ray diffraction analysis; these operations are shown in the tenth and eleventh frames, respectively.

The next operation is the stacking of the platelets in the desired sequence to form the desired assembly. This operation, shown in the twelfth picture, takes place in a Fed Std 209, Class 10,000 clean room under Class 100 laminar flow benches.

Diffusion bonding of the assembled platelet stack is performed in vacuum hot presses, specifically designed for this process. Aerojet has three such furnaces, one of which is shown in the thirteenth frame of Figure B4. These furnaces raise the assembly to the bonding temperature while applying a compressive, uniaxial load. Performed under a non-oxidizing environment, usually vacuum, this solid state process fuses the individual platelet layers together. The result of this process is the formation of an essentially monolythic device having the characteristics of the parent material but containing a potential myriad of passageways.

Following diffusion bonding, the assembly is generally proof and leak tested and may be subject to additional inspection operations such as ultrasonic or Cat Scan.

Quite commonly, secondary operations such as machining and / or forming are performed on the bonded platelet assemblies to complete the required component fabrication. Photoes of a platelet panel in its flat bonded state and then in its subsequently three dimensionally formed state are shown in the last two frames of Figure B4.

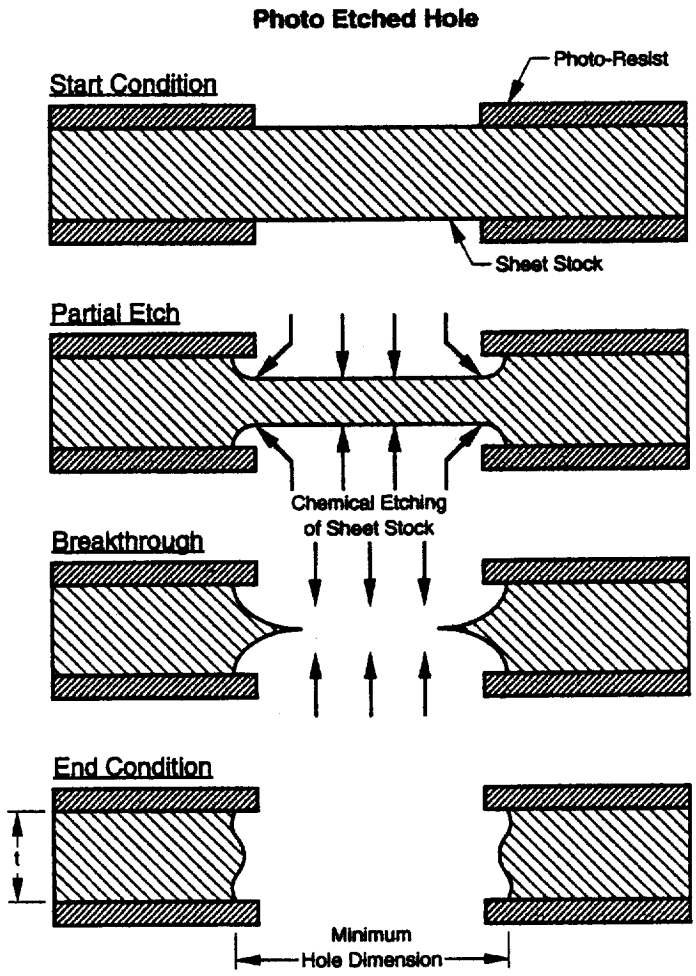

Figure B1. The Platelet Etching Process

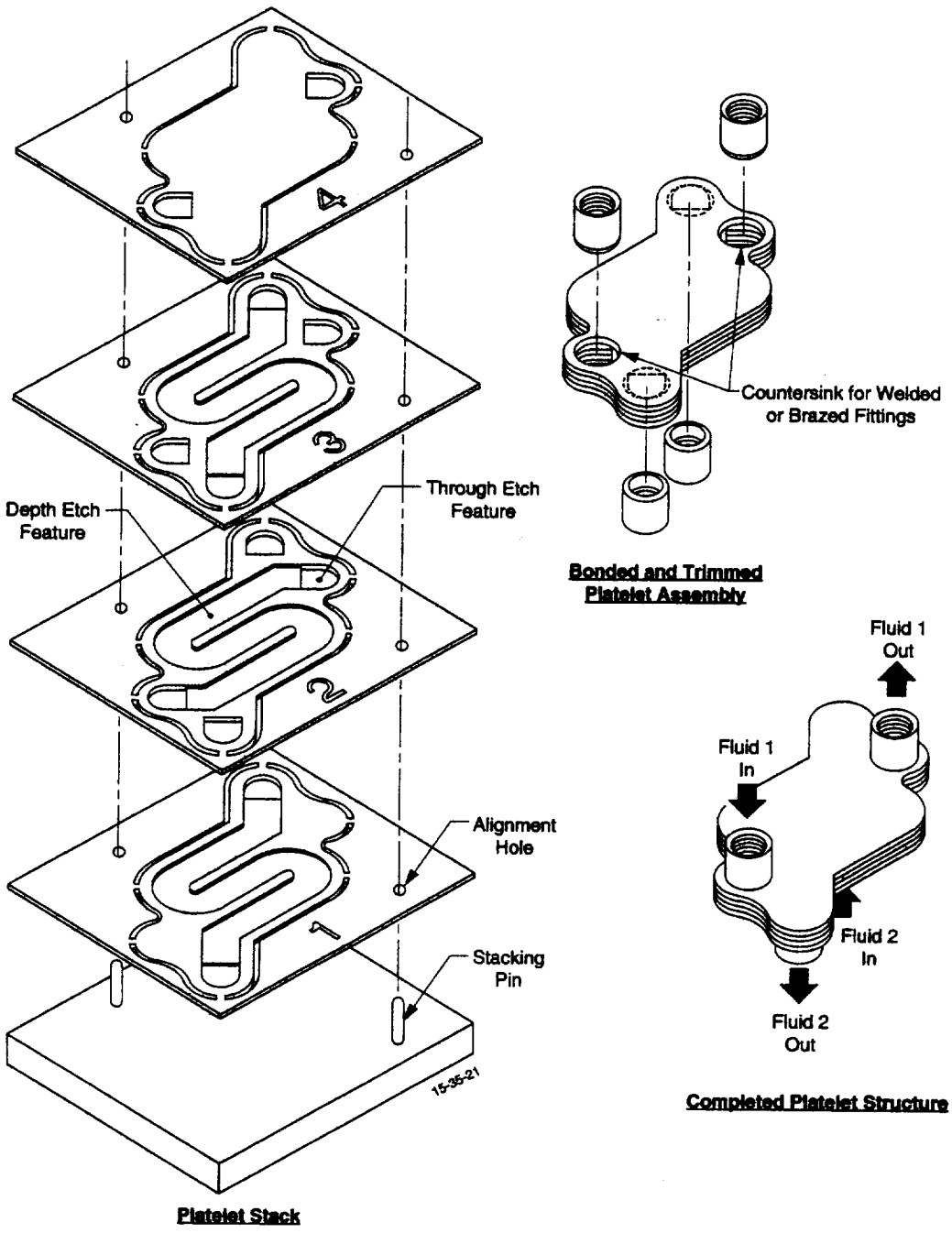

Figure B2. Platelet Device Assembly

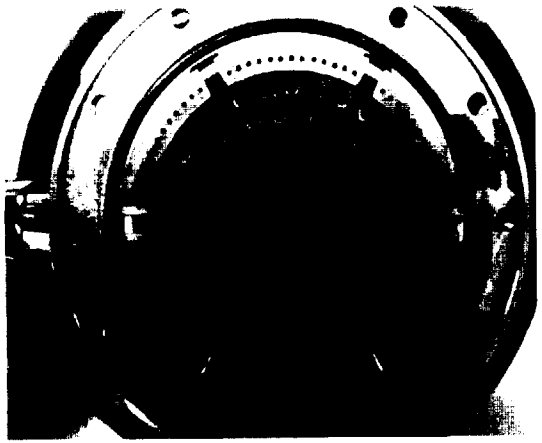

Rocket Injector

Hypersonic Engine Strut

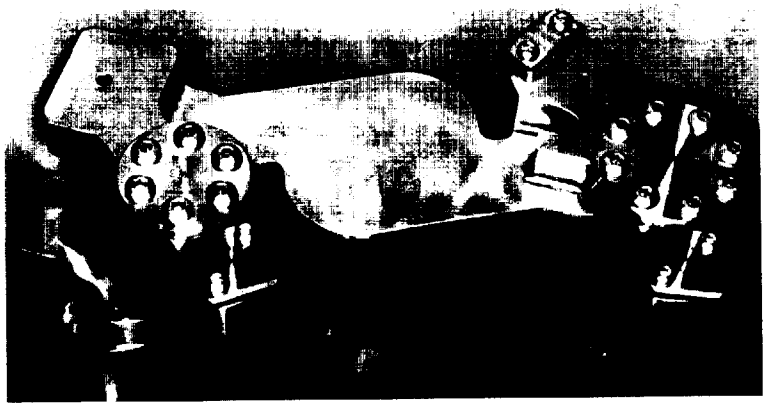

Heat Exchanger

Combustion Chamber

Figure B3. Typical Platelet Devices

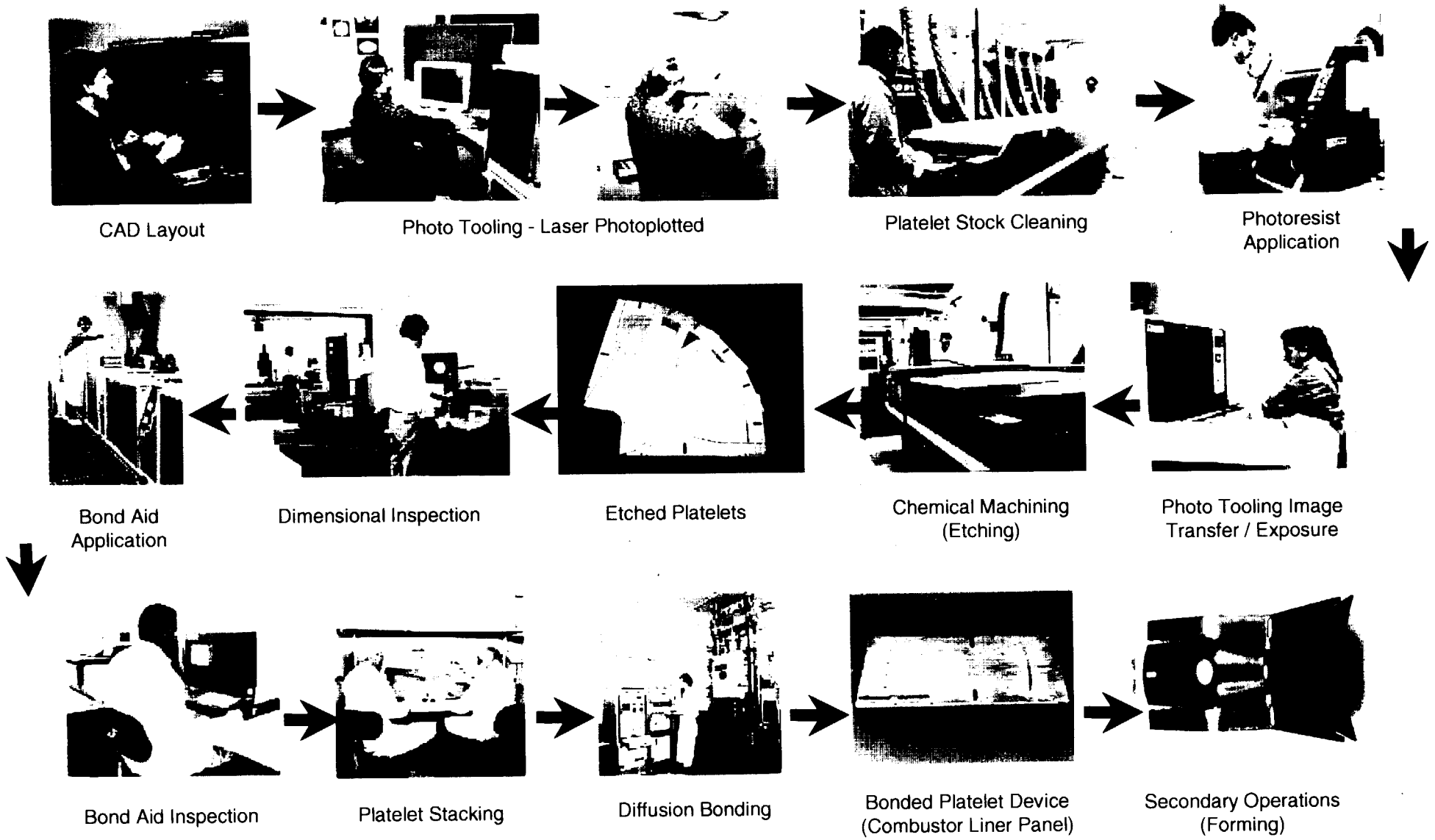

Figure B4 Platelet Device Design and Fabrication Process